Electronic Supplementary Material (ESI) for Physical Chemistry Chemical Physics.

Supplementary Information

High-concentration $LiPF_6$/sulfone electrolytes: structure, transport properties, and battery application

Yosuke Ugata,[†, ‡] Yichuan Chen,[†] Shuhei Miyazaki,[†] Shohei Sasagawa,[†] Kazuhide Ueno,[†, ‡] Masayoshi Watanabe,[‡] and Kaoru Dokko *[, †, ‡]

[†]Department of Chemistry and Life Science, Yokohama National University, 79-5 Tokiwadai, Hodogaya-ku, Yokohama, Kanagawa 240-8501, Japan

[‡]Advanced Chemical Energy Research Center, Institute of Advanced Sciences, Yokohama National University, 79-5 Tokiwadai, Hodogaya-ku, Yokohama, Kanagawa 240-8501, Japan

*CORRESPONDING AUTHOR

E-mail address: dokko-kaoru-js@ynu.ac.jp (K.D.)

Phase Behaviors and Solvate Structures

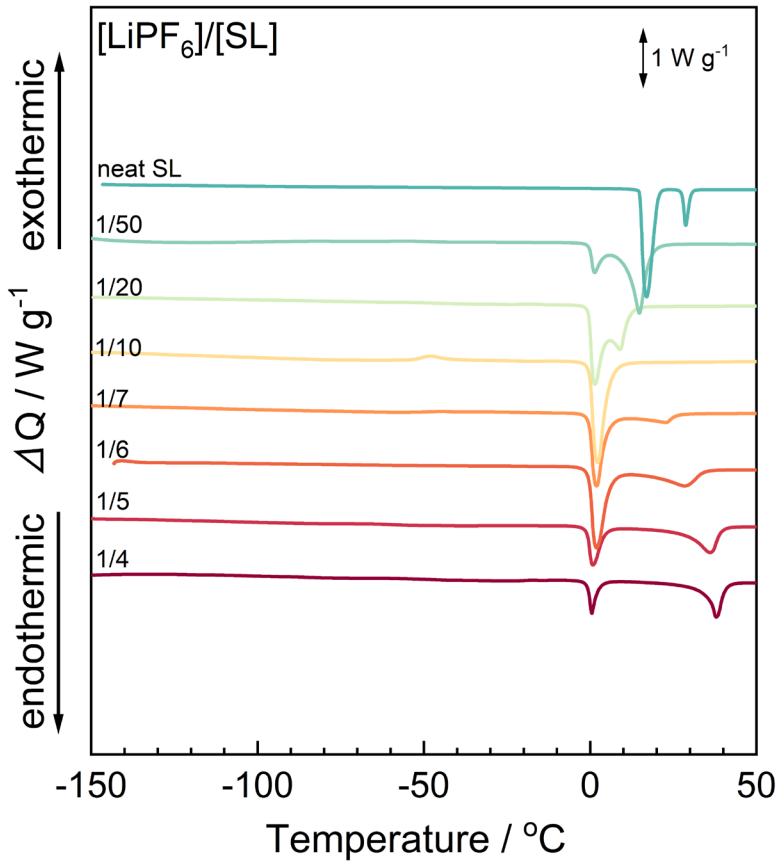

Figure S1. Differential scanning calorimetry (DSC) thermograms of $LiPF_6$–sulfolane (SL) binary mixtures.

Purified lithium triflate (LiOTf), lithium difluoro(oxalato)borate (LiDFOB), and sulfolane (SL) were purchased from Kishida Chemical and used as received. Li salts and sulfone solvents were mixed in an Ar-filled glovebox (VAC, [H_2O] < 1 ppm), and the mixtures were stirred at room temperature for 24 h. Some of the mixtures with higher melting points were heated on a hot plate to 100 °C until they turned homogeneous.

The LiOTf−SL mixture showed eutectic behavior (**Figure S2**). At $X_{LiOTf} > 0.09$, the T_m of LiOTf−SL mixture increased with increasing mole fraction of LiOTf, indicating the formation of stable solvates at a certain composition. The LiOTf−SL mixtures at larger LiOTf mole fractions ($X_{LiOTf} > 0.25$) solidify even at elevated temperatures (~60 °C), probably due to the high T_m of the solvate or low solubility of the LiOTf salt. Single crystals of an SL solvate of LiOTf [Li(SL)OTf] were successfully grown in a 1:4 molar mixture of [LiOTf]/[SL] at room temperature.

The LiDFOB−SL mixture also showed eutectic behavior. In this case, T_m increased gradually as X_{LiDFOB} increased in the range of $0.09 \leq X_{LiDFOB} \leq 0.33$, suggesting that LiDFOB forms a stable solvate with SL at a 1:2 molar ratio.

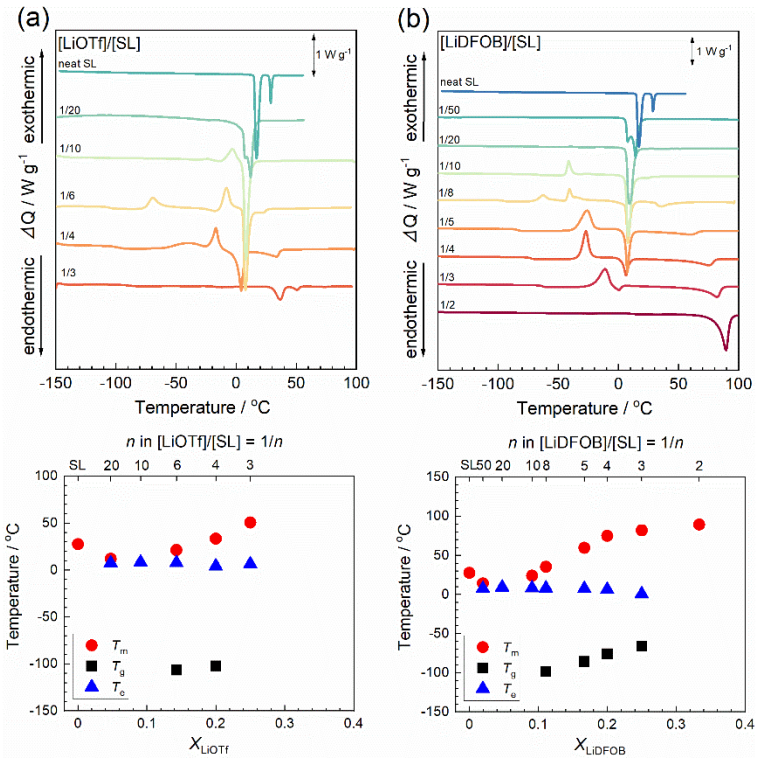

Figure S2. DSC thermograms and phase diagrams of (a) lithium triflate (LiOTf)−SL and (b) lithium difluoro(oxalate)borate (LiDFOB)−SL binary mixtures. X_{LiOTf} and X_{LiDFOB} are mole fractions of LiOTf and LiDFOB, respectively.

Table S1. Crystallographic data of $[LiPF_6]/[SL] = 1/4$ and $[LiOTf]/[SL] = 1/1$

	$[LiPF_6]/[SL] = 1/4$	$[LiOTf]/[SL] = 1/1$
Chemical formula	$C_{16}H_{32}F_6LiO_8PS_4$	$C_5H_8F_3LiO_5S_2$
Formula weight	632.56	276.15
Crystal system	monoclinic	monoclinic
Space group	$P\,1\,2_1/n\,1$ (No. 14)	$I\,1\,2/a\,1$ (No. 15)
a / Å	16.7168(7)	8.5408(8)
b / Å	8.3892(3)	23.905(2)
c / Å	19.5667(8)	10.7593(8)
α / °	90	90
β / °	100.287(4)	91.014(7)
γ / °	90	90
V / Å^3	2699.94(19)	2196.4(3)
Z	4	8
D_{calc} / g cm^{-3}	1.556	1.670
μ / mm^{-1}	0.491	0.527
Temp. / K	223	223
Reflections collected	40449	10872
Independent reflection, R_{int}	7333, 0.0266	2380, 0.0330
R_1 [$I > 2\sigma(I)$]	0.0407	0.0568
wR_2 (all data)	0.1187	0.1631
Goodness of fit	1.022	1.015

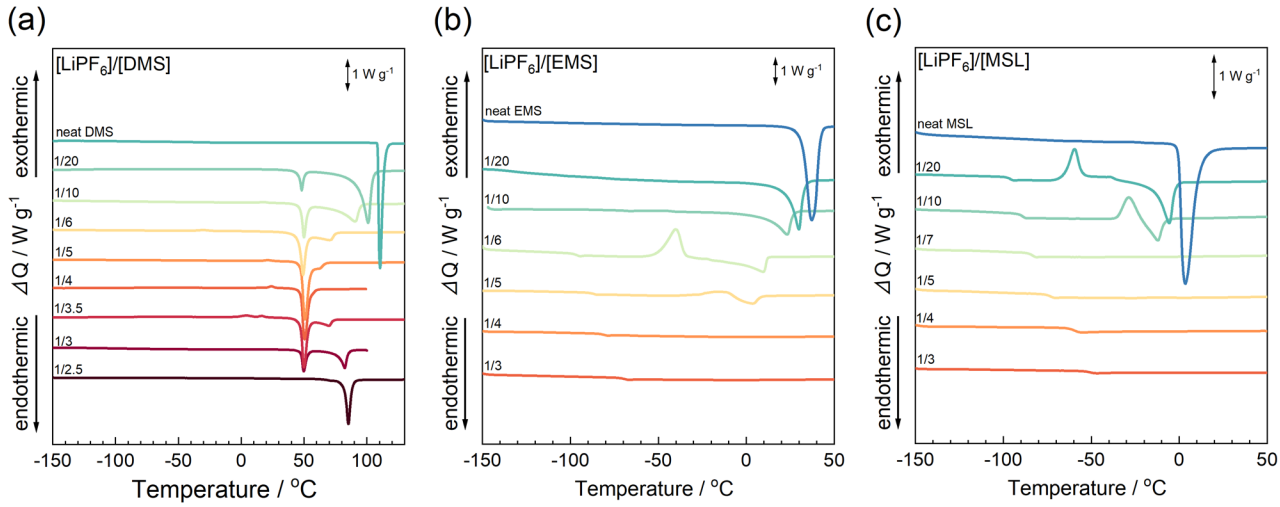

Figure S3. DSC thermograms of the binary mixtures of $LiPF_6$ and (a) dimethyl sulfone (DMS), (b) ethyl methyl sulfone (EMS), and (c) 3-methyl sulfolane (MSL).

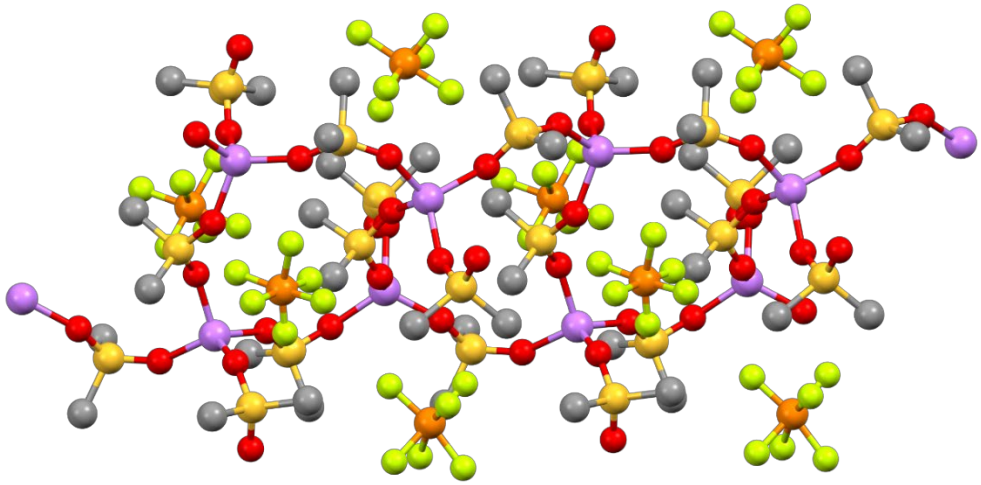

Figure S4. Ball-and-stick model of the crystal of $[LiPF_6]/[DMS] = 1/2.5$. Color code: purple, Li; red, O; gray, C; light green, F; orange, P. Hydrogen atoms are not shown. The crystallographic information file (CIF) for $[LiPF_6]/[DMS] = 1/2.5$ has not been deposited in the Cambridge Structural Database. A single crystal of the solvate of $[LiPF_6]/[DMS] = 1/2.5$ was grown in the mixture of $[LiPF_6]/[DMS] = 1/3$ at room temperature.

Table S2. Crystallographic data of $[LiPF_6]/[SL] = 1/2.5$

	$[LiPF_6]/[SL] = 1/2.5$
Chemical formula	$C_{10}H_{30}F_{12}Li_2O_{10}P_2S_5$
Formula weight	774.48
Crystal system	orthorhombic
Space group	*Pccn* (No. 56)
a / Å	22.5958(15)
b / Å	13.0371(10)
c / Å	10.4932(7)
α / °	90
β / °	90
γ / °	90
V / Å^3	3091.1(4)
Z	8
D_{calc} / g cm^{-3}	1.664
μ / mm^{-1}	0.590
Temp. / K	223
Reflections collected	25402
Independent reflection, R_{int}	4241, 0.0569
R_1 [$I > 2\sigma(I)$]	0.0493
wR_2 (all data)	0.1138
Goodness of fit	1.135

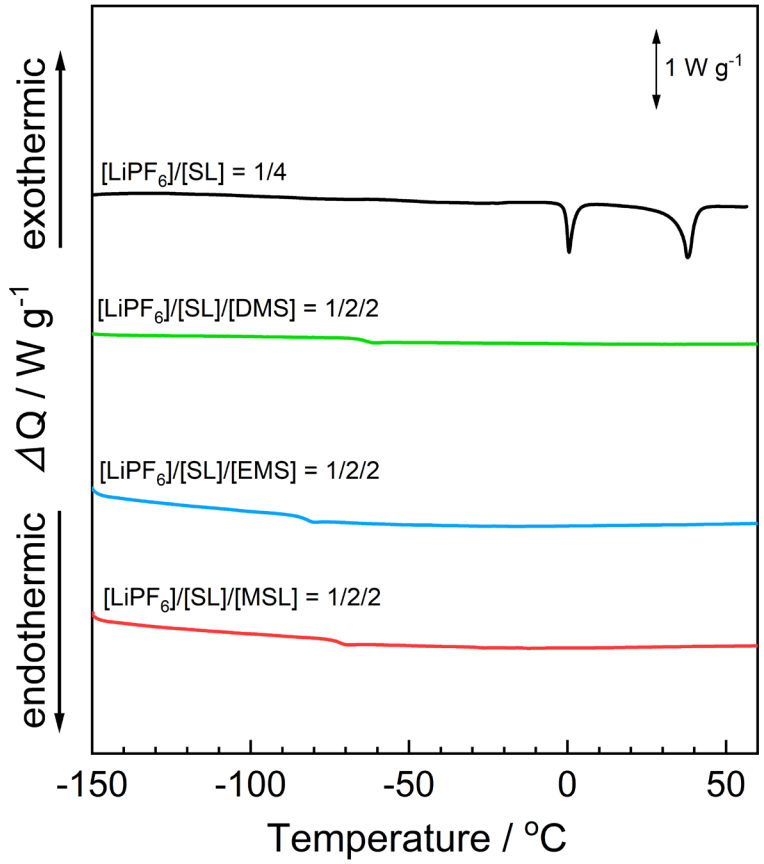

Figure S5. DSC thermograms of [$LiPF_6$]/[SL] = 1/4 and [$LiPF_6$]/[SL]/[another sulfone] = 1/2/2.

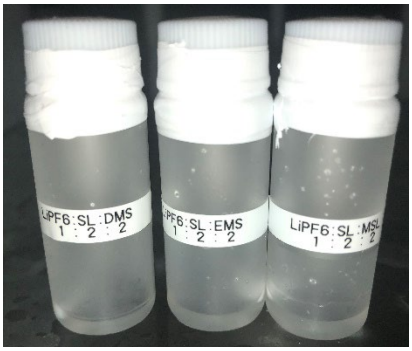

Figure S6. Photograph of the ternary mixtures of [$LiPF_6$]/[SL]/[another sulfone] = 1/2/2 after one month of storage in a −20 °C freezer.

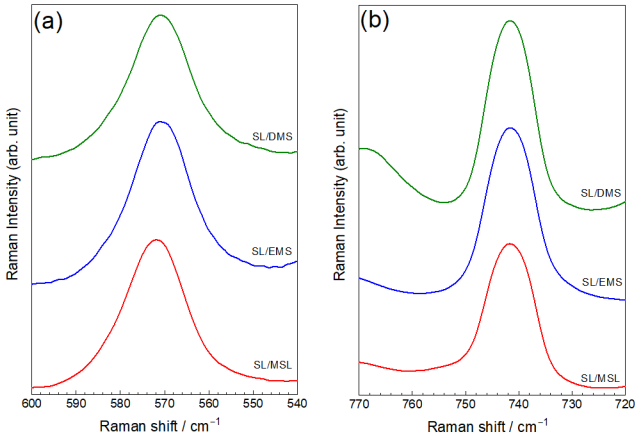

Figure S7. Raman spectra in the regions of the (a) SO_2 scissoring mode of SL and (b) P−F symmetric stretching mode of PF_6^- in the ternary mixtures of [$LiPF_6$]/[SL]/[DMS] = 1/2/2, [$LiPF_6$]/[SL]/[EMS] = 1/2/2, and [$LiPF_6$]/[SL]/[MSL] = 1/2/2.

Physicochemical Properties of the Binary $LiPF_6$–Sulfone Electrolytes

Table S3. Viscosity (η), density (ρ), $LiPF_6$ concentration (c), ionic conductivity (σ), and self-diffusion coefficients (D) of the $LiPF_6$–MSL electrolytes at 30 °C

[MSL]/[$LiPF_6$]	η	ρ	c	σ	D_{Li}	D_{sol}	D_{anion}
	mPa s	g cm^{-3}	mol dm^{-3}	mS cm^{-1}	10^{-7} cm^2 s^{-1}		
3	1106	1.38	2.49	0.27	0.22	0.16	0.16
4	316	1.35	1.95	0.64	0.60	0.54	0.54
6	88	1.30	1.36	1.34	1.66	1.78	1.90
8	48	1.26	1.03	1.73	-	-	-
10	34	1.26	0.84	1.92	3.28	4.30	4.50
20	18	1.22	0.43	1.68	-	-	-

Table S4. Viscosity (η), density (ρ), $LiPF_6$ concentration (c), ionic conductivity (σ), and self-diffusion coefficients (D) of the $LiPF_6$–EMS electrolytes at 30 °C

[EMS]/[$LiPF_6$]	η	ρ	c	σ	D_{Li}	D_{sol}	D_{anion}
	mPa s	g cm^{-3}	mol dm^{-3}	mS cm^{-1}	10^{-7} cm^2 s^{-1}		
3	1076	1.41	2.96	0.31	0.17	0.22	0.18
4	271	1.36	2.33	0.75	0.47	0.69	0.60
6	66	1.30	1.63	1.90	1.95	3.05	2.77
8	34	1.27	1.25	2.45	-	-	-
10	24	1.25	1.02	2.68	3.86	6.89	6.19
20	12	1.22	0.52	2.70	-	-	-

Table S5. Viscosity (η), density (ρ), concentration of $LiPF_6$ (c), ionic conductivity (σ), and self-diffusion coefficients (D) of the $LiPF_6$–SL electrolytes at 30 °C

[SL]/[$LiPF_6$]	η	ρ	c	σ	D_{Li}	D_{sol}	D_{anion}
	mPa s	g cm^{-3}	mol dm^{-3}	mS cm^{-1}	10^{-7} cm^2 s^{-1}		
6	78	1.38	1.59	2.03	2.14	2.06	2.29
8	42	1.35	1.22	2.50	-	-	-
10	32	1.34	0.99	2.70	4.12	4.91	5.18
20	18	1.30	0.51	2.50	-	-	-
50	13	1.28	0.21	1.36	-	-	-

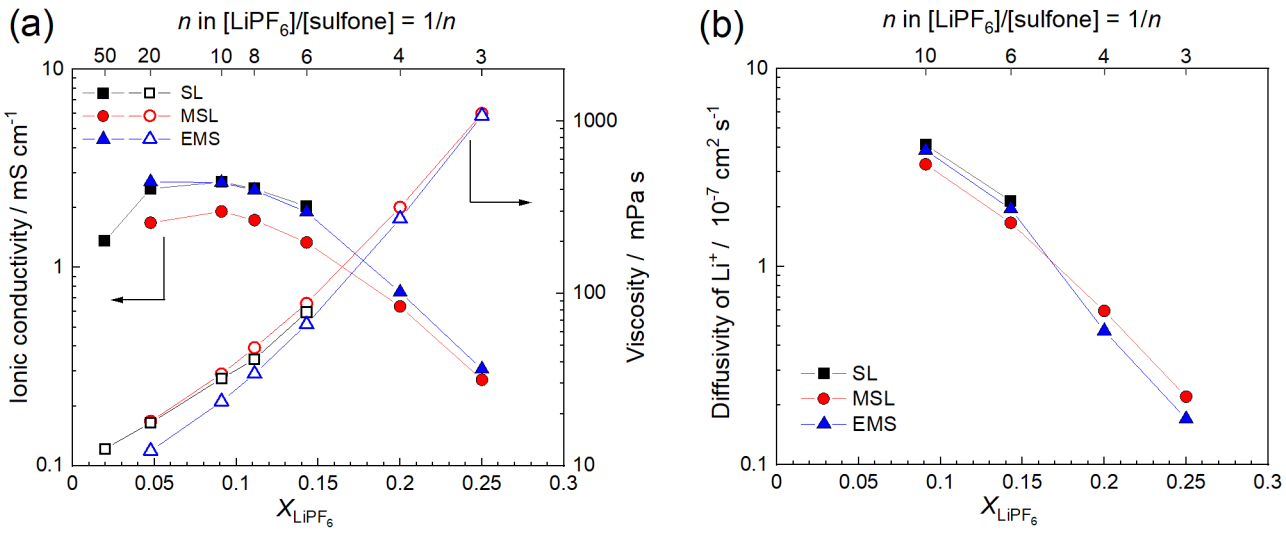

Figure S8. (a) Ionic conductivity and viscosity and (b) diffusivity of Li^+ in the $LiPF_6$–SL, $LiPF_6$–MSL, and $LiPF_6$–EMS binary electrolytes at 30 °C as a function of the mole fraction of $LiPF_6$ (X_{LiPF6}).

Physicochemical Properties of the Ternary Electrolytes

Table S6. Viscosity (η), density (ρ), $LiPF_6$ concentration (c), ionic conductivity (σ), and self-diffusion coefficients (D) of the $LiPF_6$–SL–DMS electrolytes at 30 °C. The molar ratio of SL and DMS in the ternary electrolyte was set to 1:1.

[SL+DMS]/[Li]	η	ρ	c_{Li}	σ	D_{Li}	D_{SL}	D_{DMS}	D_{PF6}
	mPa sg	cm^{-3}	mol dm^{-3}	mS cm^{-1}	10^{-7} cm^2 s^{-1}	10^{-7} cm^2 s^{-1}	10^{-7} cm^2 s^{-1}	10^{-7} cm^2 s^{-1}
4	303	1.44	2.48	0.88	0.64	0.60	0.74	0.55

Table S7. Viscosity (η), density (ρ), $LiPF_6$ concentration (c), ionic conductivity (σ), and self-diffusion coefficients (D) of the $LiPF_6$–SL–EMS electrolytes at 30 °C. The molar ratio of SL and EMS in each ternary electrolyte was set to 1:1.

[SL+EMS]/[Li]	η	ρ	c_{Li}	σ	D_{Li}	D_{SL}	D_{EMS}	D_{PF6}
	mPa sg	cm^{-3}	mol dm^{-3}	mS cm^{-1}	10^{-7} cm^2 s^{-1}	10^{-7} cm^2 s^{-1}	10^{-7} cm^2 s^{-1}	10^{-7} cm^2 s^{-1}
4	236	1.40	2.29	0.90	0.71	0.83	0.88	0.80
6	72	1.35	1.61	1.91	2.03	2.46	2.64	2.36
10	26	1.30	1.00	2.72	4.31	5.78	6.27	5.94

Table S8. Viscosity (η), density (ρ), $LiPF_6$ concentration (c), ionic conductivity (σ), and self-diffusion coefficient (D) of the $LiPF_6$–SL–MSL electrolytes at 30 °C. The molar ratio of SL and MSL in each ternary electrolyte was set to 1:1.

[SL+MSL]/[Li]	η	ρ	c_{Li}	σ	D_{Li}	D_{SL}	D_{MSL}	D_{PF6}
	mPa sg	cm^{-3}	mol dm^{-3}	mS cm^{-1}	10^{-7} cm^2 s^{-1}	10^{-7} cm^2 s^{-1}	10^{-7} cm^2 s^{-1}	10^{-7} cm^2 s^{-1}
4	292	1.39	2.10	0.78	0.63	0.66	0.58	0.60
6	82	1.34	1.46	1.64	1.87	2.04	1.78	1.91
10	34	1.29	0.91	2.23	3.32	4.78	4.17	4.53

The Li^+ ion transference numbers in the electrolytes were evaluated through a potentiostatic polarization method[S1,S2] using Li/Li symmetric cells. The metallic Li electrodes (⌀ = 16 mm, Honjo Metal), glass fiber filter separator (⌀ = 17 mm, GA-55, Advantec), and electrolyte (80 μL) were assembled in a 2032 type coin cell in an Ar-filled glovebox. The measurements were conducted with a constant voltage (ΔV) of 10 mV. Alternating current (AC) impedance measurements were conducted from 100 kHz to 100 mHz at an amplitude of 10 mV before and after the polarization of the symmetric cells. The Li^+ ion transference number (t_{Li+}^{abc}) of an electrolyte under anion-blocking conditions was estimated using the following equation proposed by Balsala et al.:[S3]

$$t_{\mathrm{Li+}}{}^{\mathrm{abc}} = \frac{I_{\mathrm{ss}}\left(\Delta V - I_{\Omega}R_{\mathrm{i},0}\right)}{I_{\Omega}\left(\Delta V - I_{\mathrm{ss}}R_{\mathrm{i,ss}}\right)}$$

where I_{SS} is the steady-state current, R_b is the bulk resistance of the electrolyte solution, and $R_{i,0}$ and $R_{i,SS}$ are the initial and steady-state interfacial resistances at the Li metal electrodes, respectively. I_Ω is the ohmic current calculated using the following equation: $I_\Omega = \Delta V/(R_b + R_{i,0})$.

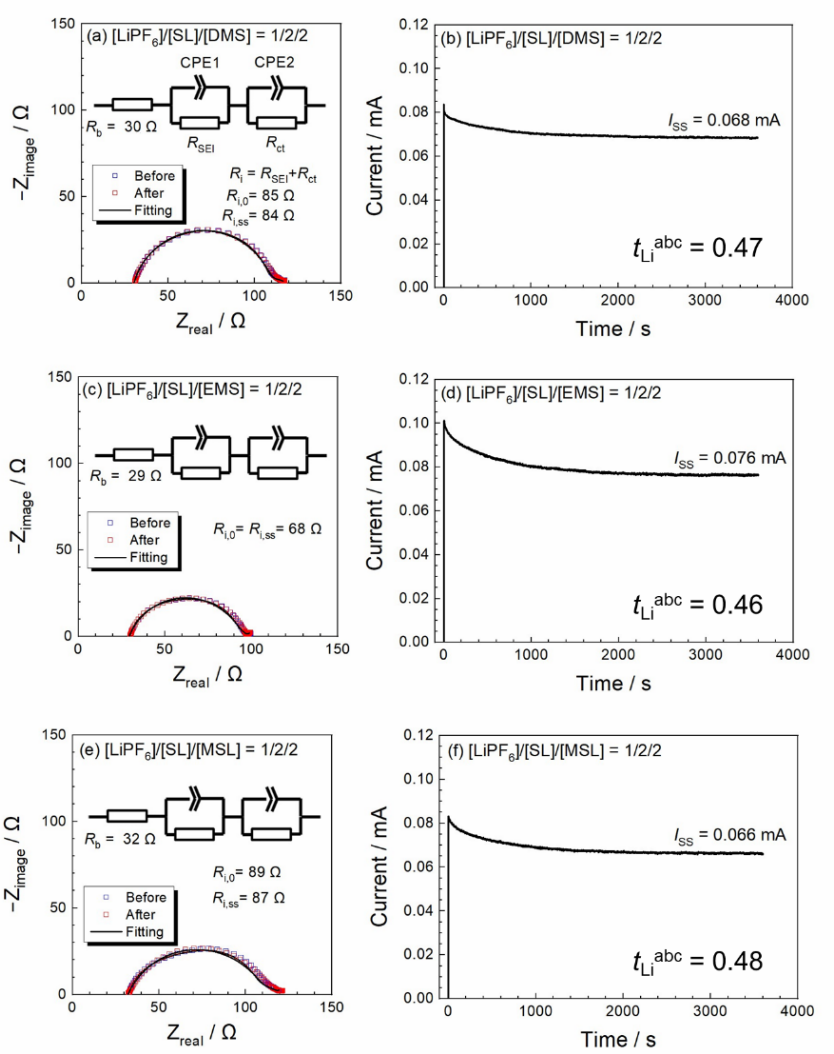

Figure S9. (a, c, e) Nyquist plots before and after polarization and (b, d, f) chronoamperometric plots of the [Li | electrolyte with glass separator | Li] cells with (a, b) [$LiPF_6$]/[SL]/[DMS] = 1/2/2, (c, d) [$LiPF_6$]/[SL]/[EMS] = 1/2/2, and (e, f) [$LiPF_6$]/[SL]/[MSL] = 1/2/2 electrolytes measured at 30 °C. The area of each Li metal electrode was 2 cm^2.

Table S9. Viscosity (η), concentration of Li salt (c_{Li}), ionic conductivity (σ), diffusivity of Li^+ (D_{Li}), and Li^+ ion transference number (t_{Li+}^{abc}) in [$LiPF_6$]/[SL]/[DMS] = 1/2/2, [$LiPF_6$]/[SL]/[EMS] = 1/2/2, and [$LiPF_6$]/[SL]/[MSL] = 1/2/2 electrolytes at 30 °C. The data for the [LiFSA]/[SL]/[DMS] = 1/2/2 and [Li salt]/[SL] = 1/4 electrolytes were obtained from Ref S4–S6.

Composition	η mPa s	c_{Li} mol dm^{-3}	σ mS cm^{-1}	D_{Li} 10^{-7} cm^2 s^{-1}	t_{Li+}^{abc} -	$\sigma \times t_{Li+}^{abc}$ mS cm^{-1}
[$LiPF_6$]/[SL]/[DMS] = 1/2/2	303	2.48	0.88	0.64	0.47	0.41
[$LiPF_6$]/[SL]/[EMS] = 1/2/2	236	2.29	0.90	0.71	0.46	0.41
[$LiPF_6$]/[SL]/[MSL] = 1/2/2	292	2.10	0.78	0.63	0.48	0.37
[LiFSA]/[SL]/[DMS] = 1/2/2	68	2.31	2.81	2.21	0.38	1.07
[LiFSA]/[SL] = 1/4	74	2.13	2.65	2.24	0.39	1.03
[LiTFSA]/[SL] = 1/4	90	1.90	1.66	1.69	-	-
[$LiClO_4$]/[SL] = 1/4	177	2.36	1.43	1.15	-	-
[$LiBF_4$]/[SL] = 1/4	100	2.36	1.32	1.60	-	-

Linear sweep voltammetry (LSV) and Cyclic voltammetry (CV)

Linear sweep voltammetry (LSV) and cyclic voltammetry (CV) were conducted using a conventional two-electrode cell setup. A Li metal disk (⌀ = 16 mm) was used as the counter electrode. The working electrodes used for LSV and CV were Pt plate (⌀ = 13 mm) and Cu foil (⌀ = 16 mm), respectively. A glass fiber filter was impregnated with the electrolyte (80 µL) and then inserted between the working and counter electrodes.

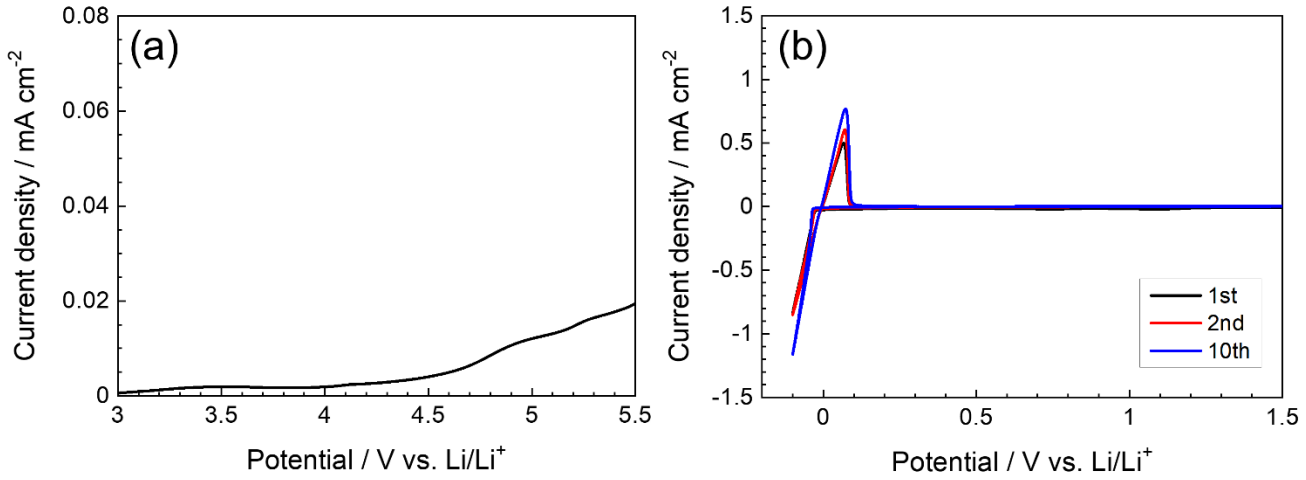

Figure S10. (a) Linear sweep and (b) cyclic voltammograms of the [$LiPF_6$]/[SL]/[DMS] = 1/2/2 electrolyte measured with Pt and Cu working electrodes, respectively. Each measurement was performed at a scan rate of 1 mV s^{-1} at 30 °C.

References

(S1) Evans, J.; Vincent, C. A.; Bruce, P. G. Electrochemical Measurement of Transference Numbers in Polymer Electrolytes. *Polymer (Guildf).* **1987**, *28*, 2324–2328.

(S2) Watanabe, M.; Nagano, S.; Sanui, K.; Ogata, N. Estimation of Li^+ Transport Number in Polymer Electrolytes by the Combination of Complex Impedance and Potentiostatic Polarization Measurements. *Solid State Ionics* **1988**, *28–30*, 911–917.

(S3) Galluzzo, M. D.; Maslyn, J. A.; Shah, D. B.; Balsara, N. P. Ohm's Law for Ion Conduction in Lithium and beyond-Lithium Battery Electrolytes. *J. Chem. Phys.* **2019**, *151*, 020901.

(S4) Ugata, Y.; Chen, Y.; Sasagawa, S.; Ueno, K.; Watanabe, M.; Mita, H.; Shimura, J.; Nagamine, M.; Dokko, K. Eutectic Electrolytes Composed of $LiN(SO_2F)_2$ and Sulfones for Li-Ion Batteries. *J. Phys. Chem. C* **2022**, *126*, 10024–10034.

(S5) Dokko, K.; Watanabe, D.; Ugata, Y.; Thomas, M. L.; Tsuzuki, S.; Shinoda, W.; Hashimoto, K.; Ueno, K.; Umebayashi, Y.; Watanabe, M. Direct Evidence for Li Ion Hopping Conduction in Highly Concentrated Sulfolane-Based Liquid Electrolytes. *J. Phys. Chem. B* **2018**, *122*, 10736–10745.

(S6) Nakanishi, A.; Ueno, K.; Watanabe, D.; Ugata, Y.; Matsumae, Y.; Liu, J.; Thomas, M. L.; Dokko, K.; Watanabe, M. Sulfolane-Based Highly Concentrated Electrolytes of Lithium Bis(Trifluoromethanesulfonyl)Amide: Ionic Transport, Li-Ion Coordination and Li-S Battery Performance. *J. Phys. Chem. C* **2019**, *123*, 14229–14238.